

A study of uranium-based multilayers: II. Magnetic properties

R Springell^{1,2}, S W Zochowski¹, R C C Ward³, M R Wells³,
S D Brown^{2,4}, L Bouchenoire^{2,4}, F Wilhelm², S Langridge⁵,
W G Stirling^{2,4} and G H Lander⁶

¹Department of Physics and Astronomy, University College London, London WC1E 6BT, UK

²European Synchrotron Radiation Facility, BP220, F-38043 Grenoble Cedex 09, France

³Clarendon Laboratory, University of Oxford, Oxford OX1 3PU, UK

⁴Department of Physics, University of Liverpool, Liverpool L69 7ZE, UK

⁵ISIS, Rutherford Appleton Laboratory, Chilton, Oxfordshire OX11 0QX, UK

⁶European Commission, JRC, Institute for Transuranium Elements, Postfach 2340, Karlsruhe, D-76125, Germany

E-mail: ross.springell@esrf.fr

Abstract. SQUID magnetometry and polarised neutron reflectivity measurements have been employed to characterise the magnetic properties of U/Fe, U/Co and U/Gd multilayers. The field dependence of the magnetisation was measured at 10K in magnetic fields from -70kOe to 70kOe. A temperature dependent study of the magnetisation evolution was undertaken for a selection of U/Gd samples. PNR was carried out in a field of 4.4kOe for U/Fe and U/Co samples (at room temperature) and for U/Gd samples (at 10K). Magnetic 'dead' layers of $\sim 15\text{\AA}$ were observed for U/Fe and U/Co samples, consistent with a picture of interdiffused interfaces. A large reduction in the magnetic moment, constant over a wide range of Gd layer thicknesses, was found for the U/Gd system ($\sim 4\mu_B$ compared with $7.63\mu_B$ for the bulk metal). This could be understood on the basis of a pinning of Gd moments arising from a column-like growth mechanism of the Gd layers. A study of the effective anisotropy suggests that perpendicular magnetic anisotropy could occur in multilayers consisting of thick U and thin Gd layers. A reduction in the Curie temperature was observed as a function of Gd layer thickness, consistent with a finite-size scaling behaviour.

PACS numbers: 61.12.Ha, 68.35.Ct, 68.65.Ac, 75.30.Cr, 75.30.Gw, 75.70.Cn

1. Introduction

The past two decades have seen a new branch of condensed matter physics develop, devoted to the investigation of multilayer thin films, driven principally by the ability to manipulate directly the electronic behaviour of materials. The tailoring of the multilayer composition and the production of samples consisting predominantly of interface regions amplify the interaction of the electronic bands with respect to the bulk layers. The study of proximity effects at the interfaces of these multilayer systems provides a route into the understanding of fundamental electronic properties. Our interest lies in the interaction of the U $5f$ electrons with those of the itinerant transition metal $3d$ states of iron and cobalt, and the more tightly bound $4f$ electrons of gadolinium.

An investigation of the structural and magnetic properties of the U/Fe system has been reported previously [1, 2], but recent modifications to the growth apparatus have allowed the introduction of Nb buffer and capping layers. Paper I in this series of articles [3] describes the fabrication and structural characterisation of U/Fe, U/Co and U/Gd multilayers grown in this way.

Earlier work on U/Fe multilayers [2] showed that the magnetism is dominated by that of the Fe atoms, and we anticipate a similar situation in the present study. Although any polarisation of the U atom is interesting, and is one of the objectives of this programme of multilayer growth, we expect any such moment to be at most $\sim 0.2\mu_B$, so that its observation requires the use of element-specific techniques, such as X-ray magnetic circular dichroism (XMCD) [4] or X-ray resonant magnetic reflectivity (XRMR) [5]. Such techniques are not discussed in the present paper. However, the influence of the uranium on the growth of the multilayers, for example its atomic size relative to the other atoms in the multilayer structure and the connection between growth and anisotropy of the magnetic layers will be reported. As shown in paper I, the growth of U/TM (TM = Fe, Co) multilayers results in a poorly defined interface which has a large amount of roughness or interdiffusion relative to the thickness of the layer. X-ray diffraction spectra indicated that the uranium was present in either an amorphous or in a poorly crystalline α -U phase. On the other hand, in the case of U/Gd both the reflectivity and high-angle X-ray diffraction results show that relatively sharp interfaces are produced, and that the uranium adopts an hcp form with a c -axis dimension not far from that of Gd, which grows in an hcp (001) preferred orientation.

This paper will address the bulk magnetic properties and to extend our knowledge of the structure within the U/TM and U/Gd multilayers. A combination of magnetometry and polarised neutron reflectivity (PNR) techniques have been used to investigate the magnetic substructure of the ferromagnetic layers, and for the case of the U/Gd system, to study the anisotropy and magnetic ordering (Curie) temperature as functions of the bilayer composition.

2. Bulk Magnetisation

This section deals with magnetisation measurements carried out on the U/TM and U/Gd multilayer systems. SQUID magnetometry measurements probe only magnetisation properties from the bulk of the sample, but it is possible to resolve effects from each of the individual components by investigating layer thickness, t , dependent properties. For the case of the U/Fe and U/Co samples, the dependence of

the saturation magnetisation on t_{Fe} and t_{Co} is presented, while for the U/Gd system, a more complete investigation has been carried out. Both t_{U} and t_{Gd} dependent studies of the ferromagnetic saturation and of the coercive field are presented. A comparison of the field dependent magnetisation measurements taken in the plane and perpendicular to the plane of the film gives a measure of the anisotropy present in these multilayers, and a zero-field cooled (ZFC) study of the magnetisation as a function of temperature, in a constant applied magnetic field, has been used to measure the Curie temperature (T_{C}) as a function of t_{Gd} .

2.1. Experimental method

The magnetisation measurements were carried out in a Quantum Design MPMS (Magnetic Property Measurement System) SQUID magnetometer both at UCL and at the Clarendon Laboratory, Oxford. The data were taken using both the DC and the reciprocating sample option (RSO) in no-overshoot mode, which enables a slow, stabilisation of the field, an important consideration when measuring ferromagnetic signals with a large diamagnetic background, as in our case, due to the relatively thick sapphire substrates. The measurements of the magnetisation as a function of applied field were recorded between -70kOe and 70kOe, at 10K, well below the Curie temperatures of iron, cobalt and gadolinium (1043K, 1388K, and 296K respectively).

2.2. U/TM Field dependence

Table 1. The saturation magnetisation values as determined by SQUID magnetometry for a selection of U/Fe and U/Co multilayer samples. Values are included for the absolute magnetisation, scaled by the respective areas and number of bilayer repeats and the values of magnetic moment per (Fe,Co) atom.

Sample Number	Composition	$t_{\text{Fe,Co}} (\pm 2\text{\AA})$	M_{sat} (emu/unit)	$M_{\text{sat}} (\mu_{\text{B}}/\text{Fe, Co})$
SN71	$[\text{U}_9/\text{Fe}_{34}]_{30}$	34	1.09E-4	1.4 ± 0.16
SN72	$[\text{U}_{23}/\text{Fe}_{17}]_{10}$	17	8.22E-6	0.2 ± 0.04
SN74	$[\text{U}_{32}/\text{Fe}_{27}]_{30}$	27	7.86E-5	1.23 ± 0.15
SN75	$[\text{U}_{35}/\text{Fe}_{27}]_{30}$	27	7.71E-5	1.2 ± 0.15
SN76	$[\text{U}_{27}/\text{Fe}_{57}]_{20}$	57	2.32E-4	1.72 ± 0.19
SN108	$[\text{U}_{28}/\text{Co}_{27}]_{20}$	27	4.38E-5	0.94 ± 0.12
SN112	$[\text{U}_{19}/\text{Co}_{19}]_{20}$	19	9.50E-6	0.30 ± 0.05
SN114	$[\text{U}_9/\text{Co}_{18}]_{20}$	18	4.44E-6	0.19 ± 0.05
SN116	$[\text{U}_{19}/\text{Co}_{42}]_{20}$	42	7.87E-5	1.10 ± 0.23

Table 1 lists the saturation magnetisation, M_{sat} in units of emu/unit, where the values given are normalised to the respective sample areas and number of bilayer repeats. Values of M_{sat} are also given in units of $\mu_{\text{B}}/\text{Fe, Co}$. Graphs of these properties are plotted as a function of $t_{\text{Fe,Co}}$ in figure 1; panel (a) describes the variation of the absolute magnetisation, while (b) plots the values of magnetic moment per atom. A straight line fit to the data in (a) can be made to describe the linear variation in absolute magnetisation, which can then be scaled in the same manner as the raw experimental data, to give the trend in saturation moment. At large values of $t_{\text{Fe,Co}}$ (insert of figure 1 (b)) M_{S} tends towards the expected bulk moment values for Fe and

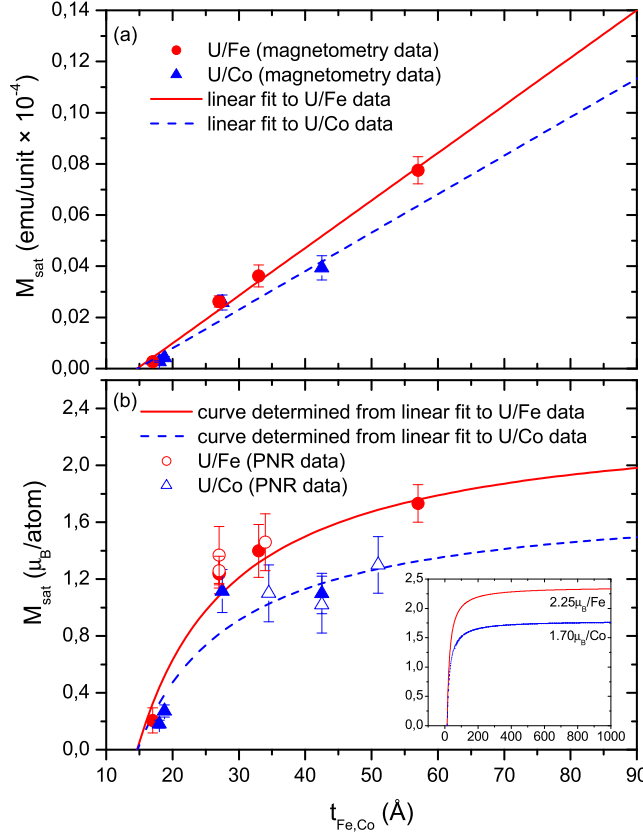


Figure 1. Variation of the saturation magnetisation, scaled by the area and number of bilayer repeats, is presented in panel (a), as a function of the ferromagnetic layer thickness. A straight-line fit is shown for both U/Fe and U/Co systems. Values of M_{sat} , given in $\mu_B/\text{Fe, Co}$, are shown in (b) and a curve is presented, calculated from the fit in (a) and extrapolated to large values of $t_{\text{Fe,Co}}$ (insert). Values of M_{sat} as determined by PNR measurements are also presented in (b).

Co of $2.2\mu_B$ and $1.7\mu_B$ respectively. The limited number of data points (figure 1 (a)) implies some uncertainty in the extremal values of M_S , although it is clear that values close to the bulk would be achieved with very thick layers. Values of the saturation magnetisation in $\mu_B/\text{Fe, Co}$, as determined by polarised neutron reflectivity, are also plotted in figure 1 (b); these measurements are described in detail later in the text.

The linear fit to M_{sat} described in figure 1 (a) shows a direct proportionality between the increase in Fe or Co layer thickness and the saturation magnetisation. The intercept of this line with the x-axis is an indication of the thickness at which there will be no magnetic moment, a magnetic 'dead' layer. However, this distinct separation of a non-ferromagnetic component and a ferromagnetic one is an unrealistic description of the Fe and Co layers. Mössbauer measurements on the U/Fe system [2] have recently been reinterpreted [3] to give an Fe layer comprising of three components, $\text{Fe}_{\text{amorphous}}$, which is paramagnetic, Fe_{bcc} carrying the bulk moment, and a non-

magnetic Fe component likely to be present in a U-Fe alloy, where the spin up and spin down $3d$ bands of the iron can be equally populated; this alloy will be present at both U | Fe and Fe | U interfaces, since one of the principal factors for the formation of these alloy regions is that of chemical interdiffusion, a process independent of the sputtering sequence.

It is not at first obvious where within the Fe layer these components form, but careful consideration of the interfacial structure from X-ray diffraction data [3] and results from Mössbauer spectroscopy [2] suggest that the centre of the layers are comprised of bulk-like Fe, provided the Fe layers are thicker than the crystalline limit, $\sim 20\text{\AA}$ [3] and then an interdiffuse U-Fe alloy region will be formed at the interfaces. These interfaces will then include components of non-magnetic Fe, where the concentrations of Fe in U are low, and hence the coordination number of Fe is low. Then, across the interface from U to Fe, as the concentration of Fe atoms increases, paramagnetic Fe will be found and then ferromagnetic Fe as crystallites of bcc Fe form. This result is supported by the X-ray diffraction data presented in Paper I [3], which shows that for sample SN72, $[\text{U}_{23}/\text{Fe}_{17}]_{10}$, there is no visible intensity from any bcc Fe component, however a small magnetic moment is still present. This result suggests that the interface is a complicated mixture of a broad spectrum of Fe components. The similar atomic size (10.3\AA^3 for Co compared with 11.5\AA^3 for Fe) and diffusion properties of cobalt are likely to result in a similar interfacial structure and this is supported by the results shown in figure 1.

Although it is not wholly accurate to assign a 'dead' layer value to a multilayer system, it is a useful tool to compare the extent of the interface from U/Fe to U/Co and to U/Gd. In the case of U/Fe and U/Co the values are very similar, $t_{\text{Fe}}^{\text{dead}}$ and $t_{\text{Co}}^{\text{dead}}$ are both $\sim 15\text{\AA}$. The formation of such interfaces in transition metal multilayers is not uncommon and has been reported in Ni/Cu [6], Fe/W [7], Fe/V [8], Fe/Nb [9] and Co/Ti [10] systems.

2.3. U/Gd Field dependence

A study of the structural properties of U/Gd multilayers [3], compared with those of U/TM systems, indicated that the U/Gd interfaces were sharper than those for U/Fe or U/Co multilayers and did not include such a significant region of interdiffusion. In this case, the magnetic 'dead' layer was expected to be small.

Values of the saturation magnetisation, M_{sat} , are summarised in table 2, in both units of emu/unit and μ_{B}/Gd , where emu/unit refers to a normalisation of M_{sat} per unit area and per bilayer. These data are shown in figure 2 (a) for samples with $t_{\text{U}} \sim 25\text{\AA}$. A linear relationship is found between the saturation magnetisation and the gadolinium layer thickness. The x-axis intercept of the fitted line gives the thickness of the magnetic 'dead' layer, which in this case is $\sim 4\text{\AA}$. Figure 2 (b) shows the variation of M_{sat} as a function of t_{Gd} in units of μ_{B}/Gd . The straight-line fit to the data in panel (a) has been scaled in the same manner as the experimental data. The inset figure in panel (b) shows the extrapolated form of the saturation magnetisation for large values of t_{Gd} , towards a value of $4.3\mu_{\text{B}}$. Figure 2 (b) also includes saturation magnetisation data obtained from polarised neutron reflectivity data (PNR), described in Section 3.

There are some important observations to be made from figure 2. First, the magnetic 'dead' layer of about 4\AA is significantly thinner than that observed in the U/TM systems. Second, whereas for the U/TM multilayers M_{sat} tended towards the bulk moment value for very thick TM layers (see insert of figure 1 (b)) the saturation

Table 2. Summary of the absolute saturation magnetisation (normalised per unit area and to the number of bilayer repeats) and M_{sat} (μ_B/Gd), for all U/Gd samples measured.

Sample Number	t_{Gd} ($\pm 2\text{\AA}$)	t_{U} ($\pm 2\text{\AA}$)	M_{sat} (emu/unit)	M_{sat} (μ_B/Gd)
SN63	33	26	3.67E-6	3.96 ± 0.48
SN64	54	26	6.04E-6	3.97 ± 0.44
SN65	76	26	8.63E-6	4.04 ± 0.42
SN66	20	39	1.74E-6	3.09 ± 0.44
SN68	20	89	1.46E-6	2.60 ± 0.37
SN120	79	29	9.32E-6	4.20 ± 0.44
SN121	38	11	4.23E-6	3.96 ± 0.46
SN122	11.4	11.1	1.03E-6	3.21 ± 0.73
SN124(600K)	24.8	10.6	2.33E-6	3.34 ± 0.46
SN134	19.8	10	2.29E-6	4.11 ± 0.62
SN135	18.2	15.8	2.02E-6	3.95 ± 0.56
SN136	19.4	19.2	2.16E-6	3.96 ± 0.56
SN137	19.5	28.2	1.96E-6	3.57 ± 0.54
SN138	20	4.8	2.67E-6	4.75 ± 0.67

magnetisation extrapolated for large values of t_{Gd} in U/Gd multilayers tends towards a value of $4.3\mu_B$, significantly reduced from the bulk metal value of $7.63\mu_B$. This indicates that the reduction in magnetic moment is not confined simply to the interface regions, but is an effect arising from the bulk of the Gd layers. Significantly reduced values of the ordered gadolinium moment have been observed in other multilayer systems, such as Gd/Mo [11], Gd/V [12] and Gd/Cr [13]. The possible mechanisms for this phenomenon were discussed for the Gd/Mo system [11] in terms of the Gd growth and pinning of the Gd moments at the interface.

In order to probe further the effect of the Gd structure on M_{sat} , a thin sputtered film of Gd was grown (sample SN62, $\sim 500\text{\AA}$ thick) under the same conditions of temperature, Ar pressure and sputtering power as the U/Gd multilayers. A value of only $\sim 5\mu_B$ was determined; this indicates that the majority of the magnetic moment reduction observed in the multilayers arises from the growth mechanism of the gadolinium layers and is not confined to the interface region. Recalling discussions presented in paper I of this series [3], for thick Gd layers large roughnesses were observed; these were described as step-like, a feature related to a columnar growth modulation. It is possible that it is at the boundaries of these column structures that the majority of the Gd moments are pinned, although some pinning will also be present at the interfaces.

It is clear, however, that the presence of the uranium layers affects the magnetisation of the gadolinium layers. In order to highlight this point figure 3 shows the saturation magnetisation values (μ_B/Gd) for a number of U/Gd samples with a constant gadolinium layer thickness of $\sim 20\text{\AA}$. As the U layers become thicker, so the saturation magnetisation decays.

A likely source of this effect is again a structural one, where variations in t_{U} can alter the internal strain within the Gd layers, which can in turn affect the pinning of the Gd moments near the U/Gd interface. A similar effect was observed in the

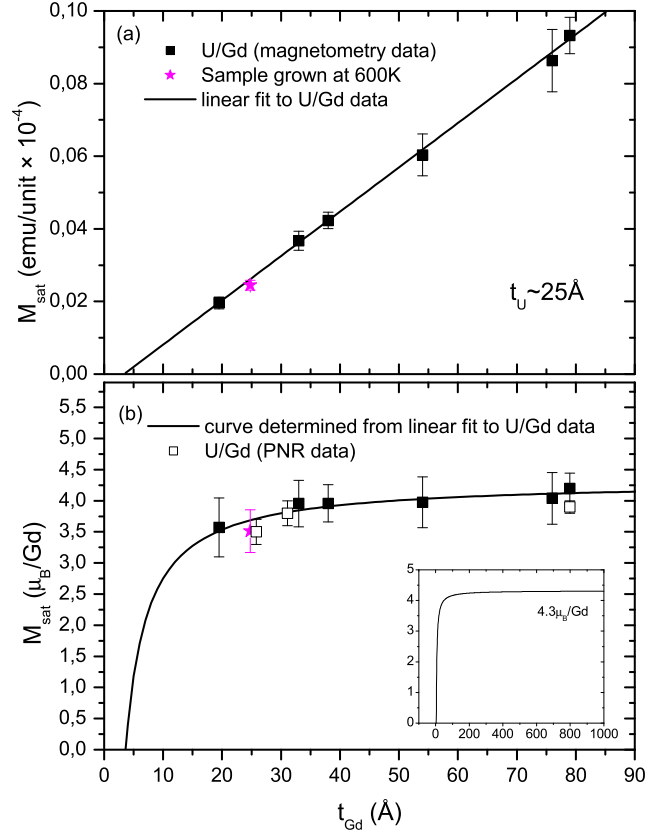


Figure 2. The variation of the saturation magnetisation, scaled by the area and number of bilayer repeats, is presented in panel (a), as a function of t_{Gd} . A straight-line fit is shown. Values of M_{sat} , given in μ_{B}/Gd , are shown in (b) and a curve is presented, calculated from the fit in (a) and extrapolated to large values of t_{Gd} (insert). The starred data points refer to sample SN124, $[\text{U}_{10.6}/\text{Gd}_{24.8}]_{20}$, grown at 600K. Values of M_{sat} as determined by PNR measurements (open squares) are also presented in (b).

Gd/Mo system [14], but in this case a linear relationship was observed between the Mo layer thickness and the reduction in Gd moment. However, the range of Mo layer thicknesses discussed was only between 7 and 15 Å, whereas in our case the U spacer layer thickness varies between 5 and 90 Å.

2.4. Anisotropy

The magnetic anisotropy is a measure of the preferred direction of the magnetisation [15], and can be determined directly from bulk magnetisation measurements, where the magnetic field is applied both perpendicular to and in the plane of the film. In this case a selected number of U/Gd samples were cut so that the measurements could be made with the samples in both orientations. The resulting hysteresis loops give values for the coercive fields, termed $H_{\text{C}}^{\text{para}}$ and $H_{\text{C}}^{\text{perp}}$ for the two magnetic field

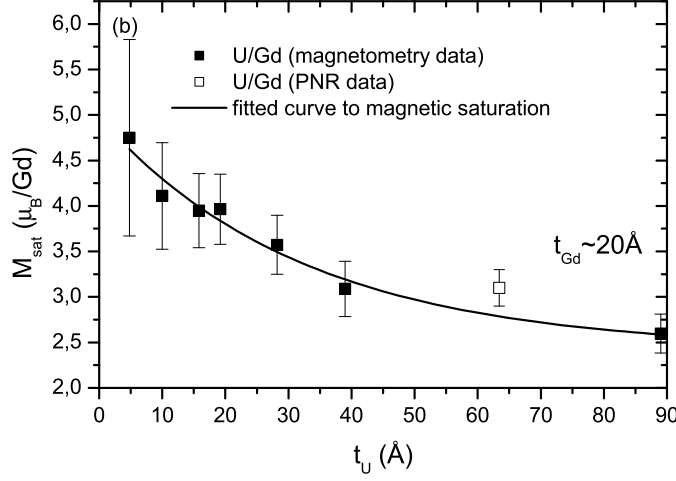


Figure 3. Values of M_{sat} are presented as a function of t_U in units of μ_B/Gd for samples with $t_{Gd} \sim 20\text{\AA}$. A PNR measurement is shown as the open square. The solid line is a guide to the eye.

directions, respectively. A discussion of the anisotropy within these systems is allied with a consideration of the values for the coercive field, since the energy involved in directing the moments along an easy axis is directly related to the applied field required to rotate them. However, it should be noted that the coercive field is also dependent on a number of other complicating factors, such as domain size and strains within the layers.

The magnetic anisotropy energy, K_{eff} can be determined from the difference in area of the magnetisation loops; this relationship holds for all directions of the magnetic easy axis. The sign convention adopted for K_{eff} , denotes that a positive K_{eff} indicates a perpendicularly oriented magnetic easy axis. This implies that the difference in area of the two loops must be taken as the subtraction of the parallel from the perpendicular loop.

The magnetic anisotropy energy or effective anisotropy is primarily a combination of magnetic dipolar (favoring an in-plane alignment) and magnetocrystalline anisotropies, stemming from the long range magnetic dipolar and spin-orbit interactions, respectively. These contributions can be resolved into volume, K_V , and surface, K_S , contributions to give,

$$K_{eff} = K_V + 2K_S/t_{Gd} \quad (1)$$

K_V is dominated by the magnetic dipolar or shape anisotropy, whereas the lowered symmetry at the interface leads to a dominant spin-orbit effect and therefore surface anisotropy. A plot of the ferromagnetic layer thickness, t , versus tK_{eff} generally yields a linear function, where the gradient of the line can be used to calculate the volume anisotropy term and the y-intercept gives twice the surface term.

Although this treatment of the anisotropy of multilayer systems has become commonplace, we note that there are several important assumptions concerning this extraction of the volume and surface contributions from the effective anisotropy. First, it is assumed that the anisotropy, localised at the interface region influences the

magnetic moments within the bulk of the layer; this is only true if the anisotropy is much smaller than the intralayer exchange. Also, the validity of the separation of the effective anisotropy into surface and volume terms becomes questionable when the layers are very thin and are almost entirely comprised of interface region. In this case, K_V is taken as independent of the thickness of the films, but it is possible in multilayer systems where the lattice mismatch between the respective species is low, to produce strain effects throughout the multilayer that introduce a magnetoelastic contribution that changes the magnetocrystalline anisotropy.

Table 3 gives H_C^{para} , H_C^{perp} and K_{eff} for selected U/Gd samples. Figure 4 (a) shows a plot of $t_{\text{Gd}}K_{\text{eff}}$ as a function of the gadolinium layer thickness and as a function of the uranium layer thickness. Panel (b) of figure 4 presents the coercive field values as a function of t_U with the applied magnetic field parallel to the plane of the sample and perpendicular.

Table 3. Summary of the coercive fields, determined from the hysteresis loops, taken with the field applied parallel and perpendicular to the plane of the film. Values of the magnetic anisotropy energy, K_{eff} , calculated as the difference in area of the hysteresis loops, measured in orthogonal field directions are also listed.

Sample	Composition	H_C^{para} (Oe) (± 10)	H_C^{perp} (Oe) (± 10)	K_{eff} (MJ/m ³) (± 0.01)
SN63	[U ₂₆ /Gd ₃₃] ₂₀	350	520	1.09
SN64	[U ₂₆ /Gd ₅₄] ₂₀	430	510	1.43
SN65	[U ₂₆ /Gd ₇₆] ₂₀	550	810	0.98
SN66	[U ₃₉ /Gd ₂₀] ₂₀	320	160	0.68
SN68	[U ₈₉ /Gd ₂₀] ₂₀	540	220	0.63
SN134	[U ₁₀ /Gd _{19.8}] ₃₀	270	670	0.92
SN135	[U _{15.8} /Gd _{18.2}] ₃₀	250	700	1.06
SN136	[U _{19.2} /Gd _{19.4}] ₃₀	240	220	1.12
SN137	[U _{28.5} /Gd _{19.5}] ₃₀	260	730	0.89
SN138	[U _{4.8} /Gd ₂₀] ₃₀	280	2270	1.26

In bulk hcp gadolinium a small uniaxial anisotropy acts to align the spins parallel to the c-axis between the magnetic ordering (Curie) temperature, $\sim 296\text{K}$, and the spin re-orientation transition temperature at $\sim 230\text{K}$. The moments then begin to tilt away from the c-axis, reaching 60° at 180K and then move back towards a canting angle of 30° at low temperatures [16]. The direction of growth of the gadolinium layers in these U/Gd multilayers has been well described [3]; the Gd layers are oriented [001], such that the uniaxial anisotropy might act to align the moments out of the plane of the film. Figure 4 (a) clearly shows that for all Gd thicknesses investigated, a negative effective anisotropy was measured. This indicates an in-plane alignment of the magnetic moments. These data points can be fitted to a straight line (shown as a dashed black line in figure 4 (a)), which has a negative slope and a positive y-intercept. These yield values for K_V and K_S of $-1.2 \pm 0.3\text{MJ/m}^3$ and $0.28 \pm 0.2\text{mJ/m}^2$, respectively, which are smaller than those obtained for the U/Fe system [17]. The negative slope indicates that the dipolar magnetic anisotropy is acting to align the moments within the plane of the film, but the positive surface contribution suggests the presence of a magnetocrystalline anisotropy, which acts to

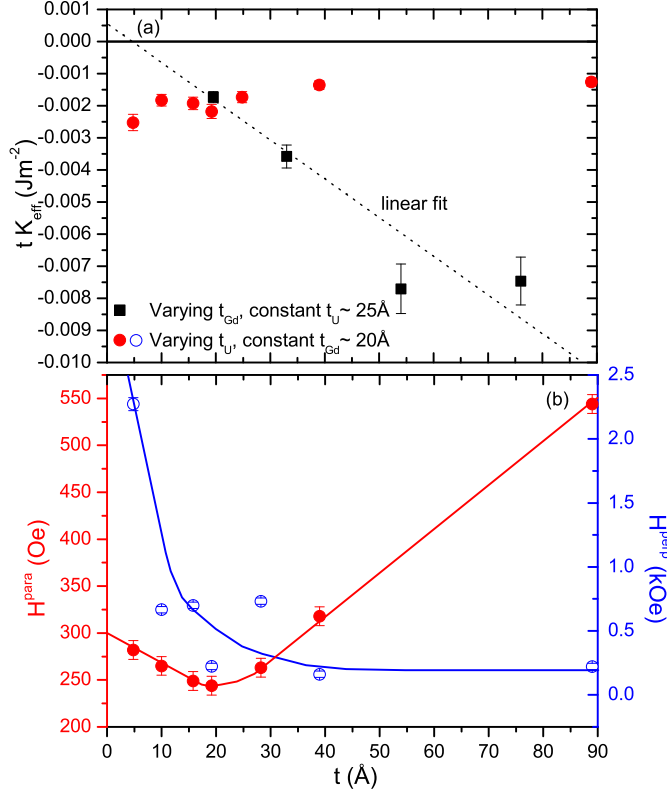


Figure 4. (a) $t_{\text{Gd}}K_{\text{eff}}$ as a function of t_{Gd} (solid black squares) and as a function of t_{U} (solid red circles). The dashed black line is a linear fit to the data. (b) coercive field values as a function of t_{U} with the applied magnetic field parallel to the plane of the sample, H_C^{para} , (left-hand y-axis, solid red circles) and perpendicular, H_C^{perp} (right-hand y-axis, open blue circles). The solid lines are guides to the eye.

align the spins perpendicularly. The line crosses the x-axis at a thickness of $\sim 5 \text{\AA}$, thus a $[\text{U}_{25}/\text{Gd}_5]_{\text{N}}$ sample might exhibit perpendicular magnetic anisotropy (PMA).

The errors on the values of K_{V} and K_{S} were relatively large and the data points at large Gd thicknesses do not fall on the line. This may be due to roughness effects, which are known to dramatically alter the anisotropy in multilayers. These have been treated theoretically [18] and have been observed experimentally in the Co/Pt system [19]. A variation from linearity at large values of t_{Gd} is consistent with the observation of increased interfacial roughness for thick Gd layers [3]. The effect of varying t_{U} on K_{eff} is of a much smaller magnitude. However, for samples with thick U layers K_{eff} tends towards more positive values, favouring an alignment of the magnetic moments perpendicular to the plane of the film.

Figure 4 (b) shows the variation in coercive field for different U layer thicknesses for both field directions. A minimum in H_C^{para} and H_C^{perp} can be observed at $t_{\text{U}} \sim 20 \text{\AA}$. As t_{U} becomes thinner H_C^{para} changes very little, whereas H_C^{perp} shows a dramatic increase. For thicker U layers the situation is the reverse; H_C^{perp} changes very little, but H_C^{para} shows a marked increase. This could be a consequence of the increased

strain, a possible explanation for the decrease in M_{sat} seen in figure 3, which would lead to a more difficult rotation of domains within the plane of the film.

2.5. Temperature dependence

The temperature dependence of the magnetisation has been measured for a number of U/Gd multilayer samples with different gadolinium layer thicknesses. Zero-field cooled (ZFC) measurements were made between 5K and 375K in an applied field of 1kOe. In this way it was possible to determine the Curie temperature (T_C) of the gadolinium layers as a function of Gd layer thickness.

It is notoriously difficult to precisely determine the ferromagnetic transition (Curie) temperature from magnetisation measurements and most attempts are made to describe the paramagnetic phase, using the Curie-Weiss law for localised moments above T_C . In our case, with such a small quantity of material and a relatively large diamagnetic background from the sapphire substrate, measurements of the paramagnetic susceptibility at these temperatures would be very difficult. For the purpose of this study T_C was taken as the point at which spontaneous magnetisation begins to be observed in the temperature dependence, where the rate of change of the susceptibility variation is greatest, i.e. the maximum in the second derivative of the susceptibility.

Figure 5 (a) shows the temperature dependent magnetisation curves for a selection of U/Gd multilayers. Panel (b) then plots the Curie temperatures for each of these samples as a function of t_{Gd} . The gadolinium layer thickness in this case is presented in units of monolayers (ML), determined from X-ray diffraction measurements [3] as 2.9Å. Such a decrease in T_C is well-known in thin film systems and can be described by a finite-size scaling relationship. A similar study of the thickness-dependent Curie temperature of gadolinium grown on tungsten [20] reported a finite-size scaling effect and asserted that an observation of this effect in thin films implies a layer-by-layer growth.

$$\frac{T_C(\text{bulk}) - T_C(t_{\text{Gd}})}{T_C(\text{bulk})} = C_0 \times t_{\text{Gd}}^{-\lambda} \quad (2)$$

C_0 is an arbitrary constant, which includes contributions from interlayer coupling effects and $\lambda = 1/\nu$, where ν is the three-dimensional Ising critical exponent of the correlation length. This treatment of finite-size scaling behaviour well describes qualitatively, Ni [21], Fe [22], Co [23] and Gd [24] systems studied previously, but includes some assumptions about the nature of the system studied. The size of the magnetic moment is not taken into account and is assumed to carry an equivalent value per atom for different layer thicknesses. This requires a coherent multilayer growth with little diffusion at the interfaces.

A fitted curve, consistent with equation (3) for the finite-size scaling, is shown as a solid black line in figure 5 (b) and yields values for λ and C_0 of -1.56 and 5.75 respectively. This gives a value for the critical exponent, ν , of 0.64, which is consistent with a 3D Ising model [25] and is consistent with the relationship observed in the Gd/W thin films [20]. These values are quoted within an error of 5%, due to uncertainties in T_C and t_{Gd} . It is also noted that the presence of capping layers on thin ferromagnetic films [26] can have an appreciable effect on T_C due to modifications in the bandstructure from hybridisation effects at the interface.

For U/Gd multilayers with the thinnest gadolinium layers, the observed T_C is much higher than that expected from the finite-size scaling behaviour. This has

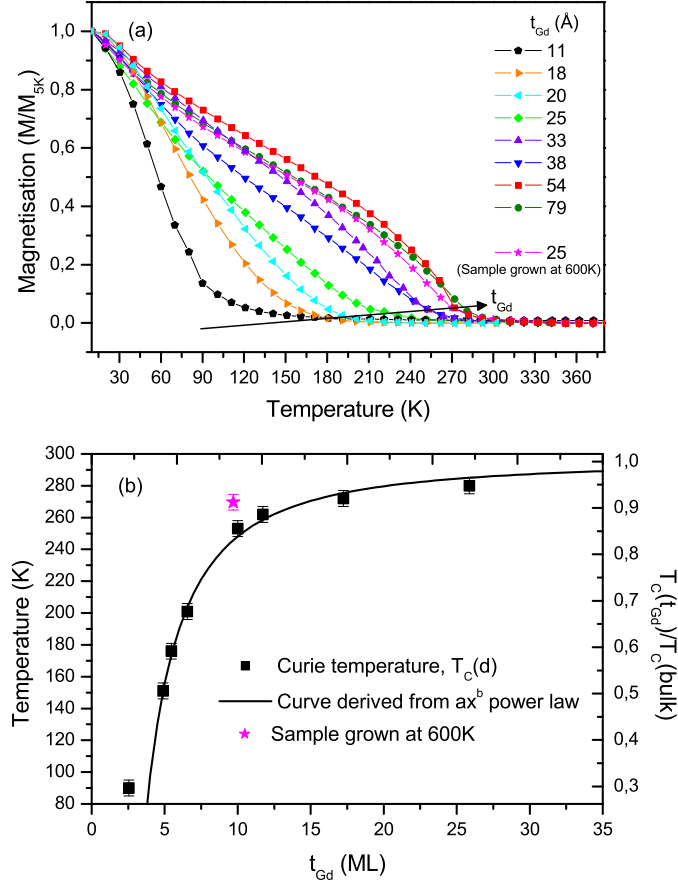


Figure 5. The temperature dependent evolution of the magnetisation in an applied magnetic field of 1kOe is shown in panel (a) for a number of U/Gd multilayer samples. The black arrow signifies the direction of increasing Gd layer thickness and the starred magenta data points are for the sample grown at an elevated substrate temperature. Panel (b) plots the Curie temperature as a function of gadolinium layer thickness. The solid black line is a fitted curve to a finite-size scaling relationship.

also been observed in the Gd/W system [20], [27] and has been related to the cross-over from 3D to 2D magnetic behaviour, where theory predicts $\nu = 1.00$ in the 2D regime. Sample SN124, grown at a temperature of 600K, also exhibits a T_C that is higher than that expected. This follows observations of the Gd/W system [20], where the increased T_C values for respective Gd layer thicknesses were attributed to the accommodation of misfit dislocations and the presence of large inhomogeneous strains, caused by steps and other defects at the interface. Previous results have shown that as the substrate temperature is increased the crystallinity is improved, but the layer roughness increases [3]. This is consistent with a columnar growth and step-like roughness profile, which could produce the effects necessary for an elevated Curie temperature.

3. Polarised Neutron Reflectivity (PNR)

Neutrons are an extremely useful tool to simultaneously study the chemical and magnetic structure, since they interact with both the nuclei and atomic moments. Polarised neutron reflectivity can be used to detect the spin-flip (SF, R^{+-} and R^{-+}) and non-spin-flip (NSF, R^{++} and R^{--}) scattering channels over a typical Q range of $0.005 - 0.25 \text{ \AA}^{-1}$. In this way, PNR can be used to determine the layer thicknesses and roughnesses, the average magnetic moment per atom, the orientation of the magnetisation and the distribution of magnetisation in magnetic multilayers.

3.1. Experimental method

PNR measurements were carried out on the CRISP reflectometer of the ISIS time-of-flight neutron source at the Rutherford Appleton Laboratories in Chilton, Oxfordshire. The CRISP instrument is situated after the liquid hydrogen moderator at 20K and analyses a wavelength band of 0.5-6.5 \AA . The neutron beam arrives at the experimental hutch at an inclination angle of 1.5° and the entrance slit provides a cross-section that is 40mm wide and between 0.5 and 6mm high. The wavelength band is defined by a disc chopper with an aperture and a nimonic chopper is used for pulse suppression. A non-adiabatic spin flipper is used to select the neutron spin direction and polarisation relaxation is suppressed by a guide field to the sample position. The sample sits approximately 10m from the moderator and reflects neutrons through two further slits to the detector, 1.75m away.

U/Fe and U/Co samples were measured at room temperature and PNR data were collected in the on-specular geometry in an applied magnetic field of 4.4kOe; large enough to saturate the magnetisation within the plane of the film. U/Gd samples were cooled (ZFC) to 10K, well below the their respective Curie temperatures. Since the measurements were made at magnetic saturation, only the NSF channels were collected. The xPOLLY programme [28] was used to calculate polarised neutron reflectivities for given samples and these were fitted to the experimental data.

3.2. Results

The following section presents the experimental data and calculated reflectivities for a selection of U/Fe, U/Co and U/Gd samples. The layer thickness and roughness parameters were fixed at values obtained from X-ray reflectometry. For the case of the U/TM multilayers the large roughnesses accounted for the diffusion at the interfaces, responsible for the magnetic 'dead' layer observed in the bulk magnetisation data. In these systems the ferromagnetic layers were separated into regions, which exhibit a magnetic moment per atom equivalent to the bulk metal, placed at the centre of the layers, and regions with no magnetic moment, at the interfaces. Although it is clear that the layers will not have such discrete sections, this technique applied to these samples was not sensitive to more complex distributions of the magnetisation.

It is possible to accurately determine the average magnetisation per atom, by closely monitoring the splitting of the two spin channels at the critical edge; the point at which the neutron transmits through the multilayer and no longer undergoes total external reflection. It is in this region of the reflectivity curve that the splitting of the two spin channels is sensitive to the magnetisation of the whole sample. The values for the average magnetic moment per atom have been displayed in figures 1 (b), 2 (b) and 3.

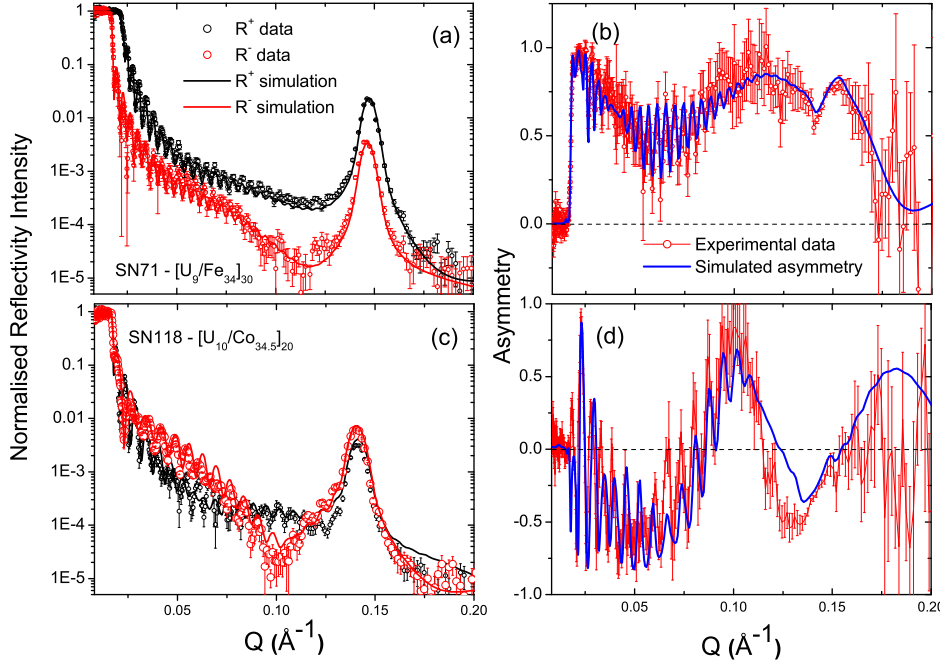


Figure 6. Panels (a) and (c) present the polarised neutron reflectivity data measured in the specular geometry at 300K and 4.4kOe for samples SN71 – $[\text{U}_9/\text{Fe}_{34}]_{30}$ and SN118 – $[\text{U}_{10}/\text{Co}_{34.5}]_{20}$, respectively. Experimental data and fitted, calculated curves are shown as black points (curve) for the R^{++} channel and red points (curve) for the R^{--} . The asymmetry for these two samples is shown in panels (b) and (d); red points represent the data and the solid blue line, the fitted calculation.

Figure 6 (a) shows the normalised non-spin-flip scattering from an example U/Fe sample, SN71 ($[\text{U}_9/\text{Fe}_{34}]_{30}$). The solid lines represent the fitted calculated reflectivities for both spin channels. Panel (b) displays the asymmetry, determined from the difference divided by the sum of the reflected intensities. Figure 6 (c) and (d) present similar results for the U/Co sample, SN118 ($[\text{U}_{10}/\text{Co}_{34.5}]_{20}$).

Table 4. The thicknesses of the three components of the transition metal layers for a selection of U/Fe and U/Co samples, determined from the fitted calculations of the PNR.

Sample	Composition	t_{TM1} (Å)	t_{TM2} (Å)	t_{TM3} (Å)
SN71	$[\text{U}_9/\text{Fe}_{34}]_{30}$	8.0	22.5	3.5
SN74	$[\text{U}_{32}/\text{Fe}_{27}]_{30}$	8.5	16.2	2.5
SN75	$[\text{U}_{35}/\text{Fe}_{27}]_{30}$	7.5	15.0	4.5
SN116	$[\text{Co}_{42}/\text{U}_{19}]_{20}$	11.0	24.0	7.0
SN117	$[\text{U}_9/\text{Co}_{51.3}]_{15}$	8.0	39.0	4.3
SN118	$[\text{U}_9/\text{Co}_{34.5}]_{20}$	8.0	22.5	4.0

A model, describing a multicomponent ferromagnetic layer in U/TM multilayers has been proposed in an earlier investigation of U/Fe multilayers [2], but a new interpretation of these components was given in paper I [3] (UTM_{alloy}|TM_{amorphous}|TM_{bulk}|TMU_{alloy}). Table 4 gives the thicknesses for a three component ferromagnetic transition metal layer. TM1 represents a combination of the UTM_{alloy} and TM_{amorphous} regions and carries no magnetic moment. It has a density that is 5% reduced from that of the bulk metal. The central region of the layer, TM2, has equivalent magnetisation and density properties to the bulk. TM3 includes the TMU_{alloy}. The calculated reflectivities and asymmetries only well reproduce the experimental data when TM1 is greater than TM3; a trend observed for all U/TM samples investigated. This is consistent with the current description of the growth of U/TM multilayers [3]. The sum of the thickness of layers TM1 and TM3 give the size of the magnetic 'dead' layer, $\sim 12\text{\AA}$, which is close to the value determined by SQUID magnetometry ($\sim 15\text{\AA}$).

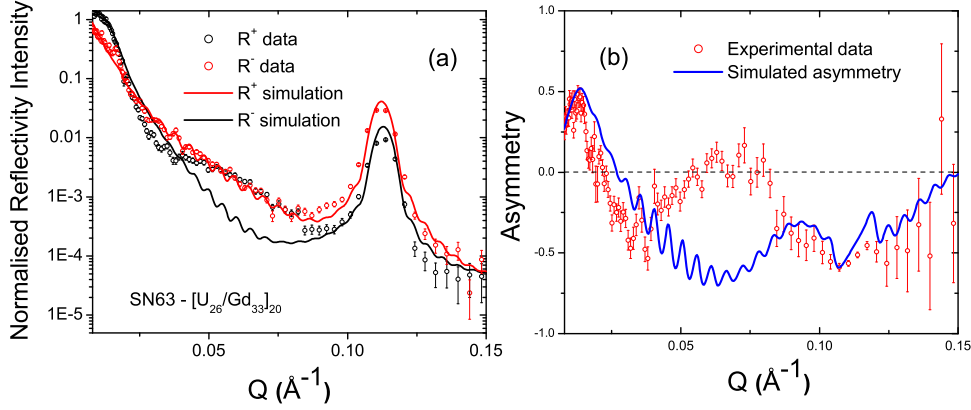


Figure 7. The polarised neutron reflectivity data (panel (a)) and the asymmetry (panel (b)), measured in the specular geometry at 10K and in an applied magnetic field of 4.4kOe are presented for sample SN63 - [U₂₅/Gd₃₃]₂₀. Experimental data and fitted, calculated curves are shown as black points (curve) for the R⁺⁺ channel and red points (curve) for the R⁻⁻. The asymmetry data is represented by red points and the fitted calculation, by the solid blue line.

Figure 7 and figure 8 show the experimental data and fitted calculations for the NSF scattering of samples SN63 ([U₂₅/Gd₃₃]₂₀) and SN124 ([U_{10.5}/Gd_{24.8}]₂₀). The latter was grown at an elevated substrate temperature of 600K.

The U/Gd samples were modelled by a simple bilayer structure. Figure 2 (b) showed that the saturation magnetisation did not vary significantly for a wide range of Gd layer thicknesses, indicating a constant distribution of the magnetisation within the Gd layers. The reduced values of the magnetic saturation calculated from SQUID magnetometry measurements were supported by those obtained from the calculated reflectivities, fitted to the PNR data. These values are listed in table 5 for a selection of U/Gd samples.

The input parameters consist of the real and imaginary parts of the neutron scattering length, b ($\times 10^{-5}\text{\AA}$), the atomic number density, N ($\times 10^{28}\text{atoms/m}^3$), the magnetic moment per atom (μ_B/atom), the angle between the moments and the applied field, θ (taken to be 0° in our case, since a magnetic field large enough to

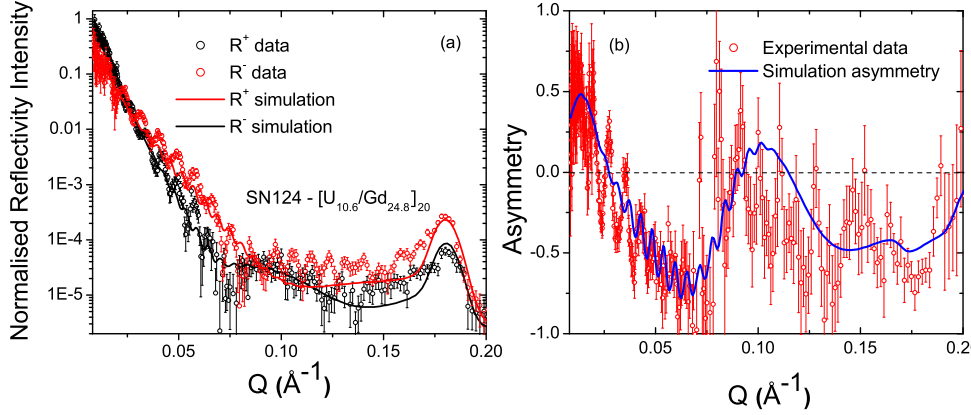


Figure 8. The polarised neutron reflectivity data (panel (a)) and the asymmetry (panel (b)), measured in the specular geometry at 10K and in an applied magnetic field of 4.4kOe are presented for sample SN124 – $[U_{10.5}/Gd_{24.8}]_{20}$. Experimental data and fitted, calculated curves are shown as black points (curve) for the R^{++} channel and red points (curve) for the R^{--} . The asymmetry data is represented by red points and the fitted calculation, by the solid blue line.

Table 5. Summary of the input parameters used to calculate the polarised neutron reflectivity data, fitted using the xPOLLY [28] programme. Values for the respective layer thicknesses, densities and magnetic moments are included.

Sample	Layer	b ($\times 10^{-5} \text{Å}$)	N ($\times 10^{28} \text{atoms/m}^3$)	t (Å)	μ_B/Gd
SN63	Gd	6.500	2.6	31.1	3.9
	U	8.417	4.8	25.0	0.0
SN65	Gd	6.500	3.0	79.0	3.8
	U	8.417	4.6	26.0	0.0
SN67	Gd	6.500	3.0	63.4	3.1
	U	8.417	4.8	20.0	0.0
SN124	Gd	6.500	2.7	24.8	3.9
	U	8.417	4.8	10.0	0.0

saturate the gadolinium layers was applied), and the layer thickness, t (Å).

It is clear from figures 7 (a) and (b) that the calculated reflectivities for the NSF channels do not well reproduce the data far away from the Bragg peak positions. In particular, the R^{--} intensity is significantly larger in this region than that calculated. This results in a large asymmetry in the calculated case, but very little splitting of the NSF channels in the experimental data. The saturation magnetisations, determined from the splitting of the channels in the vicinity of the critical edge are consistent with SQUID magnetometry measurements. These measurements indicated an even distribution of the magnetic moment through the Gd layers. It is therefore likely that the discrepancy between calculated and experimental PNR data is a product of the mechanism for the reduced magnetic moment. Attempts to introduce a complex interfacial structure, as was successful for the U/TM samples, did not result in any improvement in the fit for the U/Gd multilayers.

4. Conclusions

The magnetic properties of U/TM (Fe and Co) and U/Gd multilayers have been determined, by a combination of SQUID magnetometry and polarised neutron reflectivity measurements. These results are consistent with ideas developed in paper I [3], concerning the structure and interfacial properties of U/TM and U/Gd systems.

Magnetisation measurements on U/Fe multilayers grown on sapphire substrates with Nb buffer and capping layers, exhibited similar magnetic properties to those grown on glass [2], indicating that the predominant effects in this system arise from the interfaces of these two elements. Qualitatively similar effects were reported on the U/Co system. For large t_{Fe} and t_{Co} , values for the saturation magnetisation close to that of the bulk metals were predicted. The presence of a magnetic 'dead' layer ($\sim 15\text{\AA}$) for U/TM multilayers was determined by both SQUID magnetometry and PNR. However, it was possible to determine a further degree of complexity concerning the TM layers, from the PNR data. The experimental data were well modelled by slicing the TM layers into regions with no magnetic moment either side of a central, bulk-like region. The thicknesses of these slices were consistent with the structural description of the U/TM interfaces developed in paper I [3].

A 'missing' moment was also discovered in the U/Gd system, determined by SQUID magnetometry measurements and PNR. However, the mechanism for this reduction is clearly different from that observed in U/TM multilayers. The 'dead' layer reported in this case is $< 4\text{\AA}$; too small to account for such a large loss in magnetisation. In fact, this reduction was constant across a wide range of Gd layer thicknesses and was even observed for sputtered thin films of gadolinium. Hence, this is not an effect confined to the U/Gd interfaces, but one that is present throughout the whole of the Gd layers. A column-like growth, capable of the necessary strains and resultant defects in order to pin large numbers of Gd moments is the most likely explanation for this reduction; a picture, which is consistent with observations of the roughness and crystalline properties described in paper I [3].

A study of the anisotropy in U/Gd multilayers was carried out as a function of both t_{U} and t_{Gd} . A precise description of these trends is complex, since a large number of effects can alter the magnetic anisotropy; these effects, which commonly relate to the thickness of the respective layers, are often correlated to one another. However, the dependence of K_{eff} upon the Gd layer thickness, clearly results in a negative volume contribution and a small positive surface contribution (although the error bars are large), favouring in-plane and out-of-plane alignments of the magnetic moments, respectively. The general trend as a function of t_{U} is for an out-of plane alignment for thick U layers. Samples with thin Gd layers and thick U present a possible route towards PMA.

A close inspection of the PNR data and calculated reflectivities for the U/Gd system revealed a discrepancy between them at the half-Bragg peak positions. This feature was represented by an unusually large intensity of the R^{--} channel, compared with that calculated. Explanations at this point stem from a discussion of the mechanisms responsible for the large reduction in saturation moment; that the pinned moments at the boundaries of column-like gadolinium grains provide a certain amount of diffuse scattering, which could contribute to the intensity observed in the specular. Further PNR measurements are planned on thickness matched U/Gd samples, in order to suppress the intensity from the even order Bragg peaks and improve the sensitivity to the magnetic scattering at these positions. Off-specular measurements

are planned to investigate the diffuse scattering so that a model can be developed, which can explain such a large reduction in M_{sat} . A programme of measurements is also underway to investigate the magnetism of uranium in these multilayer systems, utilising the element-selectivity of synchrotron radiation.

Acknowledgments

RSS acknowledges the receipt of an EPSRC research studentship. We would like to thank Keith Belcher and Peter Clack of the Clarendon laboratory in Oxford and Tim Charlton and Rob Dalglish of the CRISP beamline at the ISIS neutron source.

References

- [1] A M Beesley, M F Thomas, A D F Herring, R C C Ward, M R Wells, S Langridge, S D Brown, S W Zochowski, L Bouchenoire, W G Stirling, and G H Lander. *J. Phys.: Condens. Matter*, 16:8491, 2004.
- [2] A M Beesley, S W Zochowski, M F Thomas, A D F Herring, S Langridge, S D Brown, R C C Ward, M R Wells, R Springell, W G Stirling, and G H Lander. *J. Phys.: Condens. Matter*, 16:8507, 2004.
- [3] R Springell, S W Zochowski, R C C Ward, M R Wells, S D Brown, L Bouchenoire, F Wilhelm, S Langridge, W G Stirling, and G H Lander. submitted to *J. Phys.: Condens. Matter*, 2007.
- [4] F. Wilhelm, N. Jaouen, A. Rogalev, W. G. Stirling, R. Springell, S. Zochowski, A. M. Beesley, S. D. Brown, M. F. Thomas, G. H. Lander, S. Langridge, R. C. C. Ward, and M. R. Wells. submitted to *Phys. Rev. B*, 2006.
- [5] S D Brown, A Beesley, A Herring, D Mannix, M F Thomas, P Thompson, L Bouchenoire, S Langridge, G H Lander, W G Stirling, A Mironeand R C C Ward, and S W Zochowski. *J. Appl. Phys.*, 93:6519, 2003.
- [6] J Zheng, J B Ketterson, C M Falco, and I K Schuller. *J. Appl. Phys.*, 53:3150, 1981.
- [7] J Q Xiao and C L Chen. *J. Appl. Phys.*, 70:6415, 1991.
- [8] N Hosoi, K Kawaguchi, T Shinjo, T Takada, and Y Endoh. *J. Phys. Soc. Japan*, 53:2659, 1984.
- [9] J E Mattson, C H Sowers, A Berger, and S D Bader. *Phys. Rev. Lett.*, 68:3252, 1992.
- [10] R Van Leeuwen, C D England, J R Dutcher, C M Falco, W R Bennett, and B Hillebrands. *J. Appl. Phys.*, 67:4910, 1990.
- [11] J. V. Harkins and P. E. Donovan. *J. Phys.: Condens. Matter*, 8(685), 1996.
- [12] P. Pankowski, L. T. Baczewski, T. Story, A. Wawro, K. Mergia, and S. Messoloras. *phys. stat. sol. (c)*, 1(2):405, 2004.
- [13] K. Mergia, L. T. Baczewski, S. Messoloras, S. Hamada, T. Shinjo, H. Gamari-Seale, and J. Hauschild. *Appl. Phys. A*, 74:1520, 2002.
- [14] J V Harkins and P Donovan. *J. Magn. Magn. Mater.*, 156:224, 1996.
- [15] J A C Bland and B Heinrich. *Ultrathin Magnetic Structures I*. Springer-Verlag, 1994.
- [16] S N Kaul. *Phys. Rev. B*, 62:1114, 2000.
- [17] A. Beesley. *Structural and Magnetic Studies on sputtered Uranium/Iron Multilayers*. PhD thesis, University of Liverpool, 2005.
- [18] P Bruno. *J. Phys. F*, 18:1291, 1988.
- [19] J-H Kim and S-C Shin. *J. Appl. Phys.*, 80:3121, 1996.
- [20] M. Farle, K. Baberschke, and U. Stetter. *Phys. Rev. B*, 47:11571, 1993.
- [21] F. Huang, M. T. Kief, G. J. Mankey, and R. F. Willis. *Phys. Rev. B*, 49:3962, 1994.
- [22] C. M. Schneider. *Phys. Rev. Lett.*, 64:1059, 1990.
- [23] Z. Q. Qiu, J. Pearson, and S. D. Bader. *Phys. Rev. Lett.*, 70:1006, 1993.
- [24] J. S. Jiang, D. Davidovic, D. H. Reich, and C. L. Chien. *Phys. Rev. Lett.*, 59:2596, 1995.
- [25] M S Amazonas, J Cabral Neto, and J Ricardo de Sousa. *J. Magn. Magn. Mater.*, 270:119, 2004.
- [26] P Pouloupoulos and K Baberschke. *J. Phys.: Condens. Matter*, 11:9495, 1999.
- [27] Y. Li, C. Polaczyk, and D. Riegel. *Surface Science*, 402:386, 1998.
- [28] S. Langridge. <http://www.rl.ac.uk/largescale/>.